Molded Case Electronically Assisted Circuit Breaker for DC Power Distribution Systems

Yanjun Feng, *Member, IEEE*, Xin Zhou, *Senior Member, IEEE*, Slobodan Krstic, *Member, IEEE*, Yuanfeng Zhou, *Student Member, IEEE*, and Zheng John Shen, *Fellow, IEEE*

***Abstract*—This article introduces a new dc hybrid circuit breaker (HCB) concept termed electronically assisted circuit breaker (EACB). A conventional ac mechanical molded case circuit breaker (MCCB) is used to interrupt dc fault currents with the assistance of an electronic commutation circuit, which is activated for a short time period only during the late phase of the breaking process. Unlike other prior art HCB concepts, the EACB uses a conventional thermal-magnetic MCCB baseline design with minimal modification on the actuation mechanism, arc chamber, or form factor, and uses an electronic commutation circuit, which only needs to commutate a fault current far below its peak value for a very short duration (∼100 μs), both contributing to significant cost savings. Other advantages of the EACB concept include self-powered and autonomous operation, simple installation, inherently low on-resistance, and galvanic isolation. While an EACB does not facilitate arc-free or ultrafast breaking, it does provide a simple and cost-effective way to enhance the dc current interruption capability of the conventional ac MCCBs, which currently dominate the low voltage circuit breaker market. The EACB concept has been validated both experimentally and by simulation. Several 600Vdc/250A (nominal) EACB prototypes are designed and tested. They have experimentally demonstrated a fault current interruption capability of over 8000 A at a dc voltage of 600 V within 6 ms.**

***Index Terms*—Circuit breaker, direct current (dc) power.**

I. Introduction

THE demand for cost-effective dc circuit breakers continues to grow as dc power distribution applications, such as EV charging infrastructures, PV farms, battery energy storage systems, and dc data centers further expand. Moreover, dc power offers certain advantages over traditional ac power, such as higher transfer efficiency, easier synchronous control, improved system stability and power quality, and easier integration of renewable and distributed energy resources [1], [2]. However, fault protection for dc power systems remains a major technical challenge [3], [4].

In ac power distribution systems, conventional thermal-magnetic molded case circuit breakers (MCCBs) are commonly used to provide both short circuit and overload protection. A normal current is conducted through the metal contacts of an MCCB, which are held closed by a mechanical latch. At a short circuit fault, a mechanical mechanism will release the latch under the influence of the overcurrent and let the contacts open by spring action. The MCCB relies on the electromagnetic repulsion force to respond instantaneously to a large current surge (i.e., a short-circuit fault current) or the bimetallic thermal expansion force to respond to a less stressful but longer timescale overcurrent condition. The MCCB typically provides a time–current (I^2t) response curve, and trips sooner for a larger overcurrent but endure a smaller overcurrent for a longer time, allowing a relatively large inrush current during the startup of a motor or a capacitive load. With a very large short-circuit overcurrent, the magnetic element trips the circuit breaker with no intentional delay.

However, these immensely popular and cost-effective ac MCCBs do not offer sufficient dc interruption capability due to the absence of natural current zero crossing [3]. To reduce arc damage, techniques, such as vacuum arc chamber, magnetic field assistance, or zero crossing resonant circuit were introduced [5], [6]. These techniques offer some limited improvement on their dc fault interruption capability but with a considerable penalty on complexity and cost. Solid state circuit breakers (SSCBs) [7], [8] and hybrid circuit breakers (HCBs) [9], [10] have been under intensive research to provide alternative solutions. However, the high cost and high conduction loss of semiconductor devices in the SSCBs impede its market penetration, especially in high current applications. The reported HCB solutions offer low conduction losses and a varied level of arc suppression but require a current sensing and mechanical actuation mechanism (e.g., solenoids or Thomson coils) vastly different from and far more complex than the conventional MCCBs [11]–[13]. It would be highly advantageous to develop a cost-effective solution to improve the dc fault current interruption capability of the conventional MCBs without dramatically changing their design.

In this article, we introduce a new HCB concept termed electronically assisted circuit breaker (EACB). The EACB utilizes a conventional thermal-magnetic ac MCCB and a simple electronic commutation circuit, which is only activated for a

Manuscript received June 17, 2020; revised September 14, 2020; accepted October 28, 2020. Date of publication November 11, 2020; date of current version February 5, 2021. Recommended for publication by Associate Editor V. Agarwal. *(Corresponding author: Zheng John Shen.)*

Yanjun Feng was with the Illinois Institute of Technology, Chicago, IL 60616 USA (e-mail: yfeng25@hawk.iit.edu).

Xin Zhou was with the Eaton Corporation, Pittsburgh, PA 15108 USA (e-mail: xinzhou@eaton.com).

Slobodan Krstic was with the Eaton Corporation, Milwaukee, WI 80615, USA. He is now a consultant (e-mail: krsticpowersolutions@gmail.com).

Yuanfeng Zhou and Zheng John Shen are with the Illinois Institute of Technology, Chicago, IL 60616-3717 USA (e-mail: yzhou103@hawk.iit.edu; zshen6@iit.edu).

Color versions of one or more of the figures in this article are available online at https://ieeexplore.ieee.org.

Digital Object Identifier 10.1109/TPEL.2020.3037477

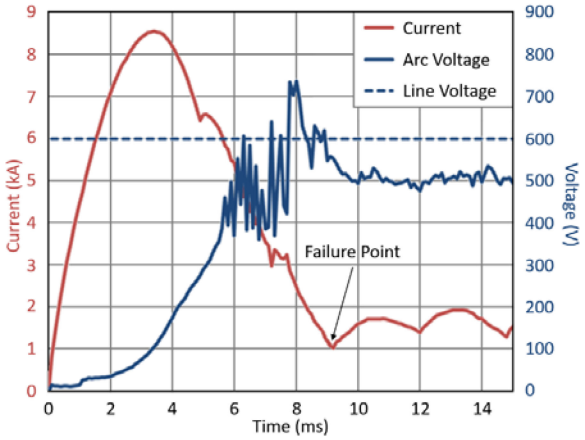

Fig. 1. Fault current and arc voltage waveforms of a failed dc fault interruption process of a conventional ac MCCB. The MCCB is able to reduce the fault current from 8500 (peak) to 1000 A (at 9 ms) but fails at that point due to the excessive heat generated from sustained arcing.

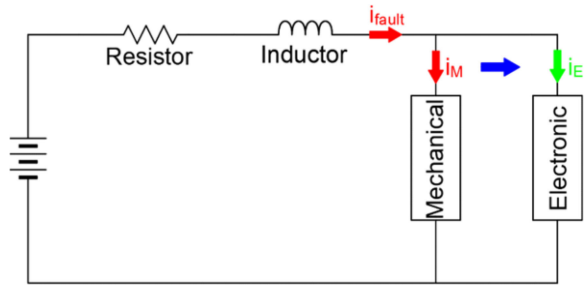

Fig. 2. Conceptual EACB schematic with two parallel mechanical and electronic paths. The mechanical path conducts the fault current most of the time during an arcing/breaking process while the fault current is momentarily commutated to the electronic path for a short time period to aid extinction of the arc in the mechanical path.

short time period (e.g., 100 μs) during the late phase of the breaker arcing/breaking process. Unlike other HCB concepts in the literature, the EACB uses the same baseline tripping and actuation mechanical design of a conventional MCCB with very little modification and no additional sensors, and uses an electronic commutation circuit with a significantly reduced current rating, both contributing to significant cost savings and easy adoption of the technology. Other advantages of EACB include self-powered and autonomous operation, simple installation, inherently low on-resistance, and galvanic isolation. While the EACB does not feature arc-free or ultrafast breaking, it does provide a simple and cost-effective way to enhance the dc current interruption capability of the conventional MCCBs currently dominating the low voltage circuit breaker market. While the basic EACB concept was recently reported in [14], this article provides additional design details and experimental results. The remainder of this article is organized as follows. Section II introduces the basic concept of EACB, whereas Section III presents the modeling and simulation results of EACB. Section IV discusses the design considerations of the EACB in detail. The experimental results are reported in Section V, followed by the conclusion in Section VI.

II. Concept of EACB

Fig. 1 shows the measured breaker current and voltage waveforms of a failed dc current interruption process of a 250 A/600 V rated conventional MCCB with a dc bus voltage of 600 V and a system time constant ($\tau = L/R$) of 1.5 ms. The fault current initially rises to 4 kA after 1 ms, when the metal contacts starts separating and causes an arc. After that, the MCCB enters the arcing/breaking process with a gradually increasing arc voltage. In the meantime, the fault current continues to increase to a peak value of 8.5 kA at 3.5 ms, and then decreases as a result of the increasing arc voltage and the loop impedance. In this particular case, the arc voltage increases to around 500 V, and the fault current decreases to 1–2 kA at 9 ms and remains at this level afterward. This indicates that the arc can no longer be extinguished, leading to the eventual destruction of the MCCB itself. The breaker fails to interrupt the dc fault current after reducing the fault current from its peak ($\sim$8.5 kA) and is very close to a successful interruption. One cannot help thinking that the MCCB might succeed in interrupting the dc fault current if some form of relief is provided to the mechanical breaker right before the failure point. This hypothesis forms the basis of the EACB concept.

The EACB has a basic configuration similar to a conventional HCB, as shown in Fig. 2, which comprises a mechanical path and an electronic path in parallel. However, there is a distinction between their operation principles. In a conventional HCB, the electronic path immediately commutates the fault current away from the mechanical switch upon the detection of a fault condition and carries the fault current almost during the entire breaking process. In an EACB, however, it is the mechanical breaker that carries the fault current during most of the arcing/breaking process while the electronic path only steps in for a very short time period during the late phase of the breaking process to aid the extinction of the arc. The EACB relies the mechanical breaker to handle most of the interruption task, and only uses the power electronic commutation circuit to provide a momentary relief to the mechanical breaker near the end. It is for this reason that the term of EACB is used to distinguish from other HCB concepts.

All the prior art HCBs commutate the fault current to the parallel electronic path shortly before or after the opening of the metal contacts, thus offer arcless or arc-light operation with an enhanced contact lifetime. However, these solutions require current sensing, tripping, and mechanical actuation designs vastly different from and far more complex than the conventional MCCB with considerable cost and size penalties. Thomson coils or special motors are used to separate the main metal contacts in these HCBs [12], [13] instead of the simple solenoid and spring mechanism used in conventional MCCBs. Furthermore, the power electronic path in these HCBs must sustain an exceedingly large fault current (e.g., up to 7 kA in the 600Vdc case study) for a few milliseconds, mandating the use of costly power semiconductor devices with extremely high current ratings. In addition, a separate mechanical isolation switch in series with

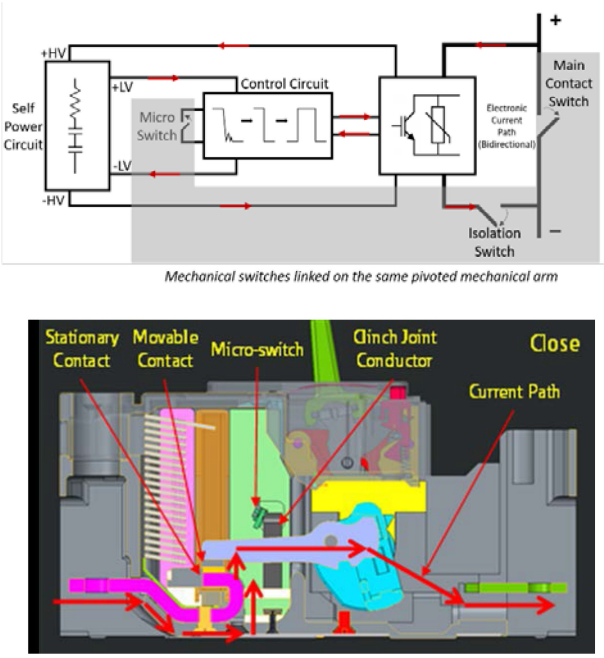

Fig. 3. Detailed EACB schematic showing the main mechanical contact switch, the isolation switch (clinch joint), and the electronic commutation circuit. The electronic commutation circuit includes IGBT switches, MOVs, a self-power circuit to draw power from the arc voltage itself to operate all the electronics, and a control and timing circuit to generate the appropriate gate signals for the IGBT. A mechanical microswitch is used to trigger the commutation operation. Note that the main contact switch, the microswitch, and the isolation switch are all part of the same mechanical arm, and open or close in synchronization one after another with a fixed delay time [23].

the HCB is required to provide galvanic isolation after the HCB fully opens.

In contrast, the proposed EACB uses the same thermal-magnetic tripping and actuation mechanisms of a conventional MCCB with only minor mechanical modifications. This will greatly reduce the complexity and cost of the EACB. In the meantime, the EACB's power electronic commutation circuit only needs to carry an already reduced fault current (1–2 kA instead of 7–8 kA) for 100–200 μs instead of 2–3 ms, leading to much lower power rating and cost than other HCB solutions. Furthermore, it offers other advantages, such as self-powered and autonomous operation, simple installation, inherently low on-resistance, and galvanic isolation. While an EACB does not facilitate arc-free or ultrafast breaking, it does provide a simple and cost-effective solution to enhance the dc current interruption capability of conventional ac MCCBs currently dominating the low voltage circuit breaker market.

Fig. 3 provides a more detailed schematic showing the major function blocks of the EACB, such as the main mechanical contact switch, microswitch, isolation switch, and electronic commutation circuit. The main mechanical contact switch conducts the load current, whereas the isolation switch cutoffs the electronic circuit and provides the required galvanic isolation after the fault current interruption is fully completed. The microswitch closes with a certain delay after the opening of the main contacts to trigger the operation of the commutation circuit. Note that the main contact switch, microswitch, and isolation switch are designed on the same pivoted mechanical arm, and open or close in synchronization one after another with fixed delay times. The mechanical arm design is very much based on that of the conventional ac breaker only with two small nonbreaking mechanical switches (micro and isolation) being added.

The electronic commutation circuit comprises an insulated gate bipolar transistor (IGBT)/metal oxide varistor (MOV) switch, a self-power circuit, and a control and timing circuit. The IGBT is the main electronic switch that conducts the fault current during the small commutation time window to relive the mechanical breaker from excessive arcing stress. The MOV in parallel with the IGBT clamps the surge voltage and absorbs the system residual electromagnetic energy when the IGBT turns OFF. There is also a diode bridge circuit connected to the IGBT and MOV to provide bidirectional current flow for the EACB. The self-power circuit draws power from the arc voltage itself to supply 30 and 5 V to all other electronic function blocks so the EACB does not need any external power supply. Note that the electronic circuit is not powered up when the mechanical breaker conducts normal load currents. The control and timing circuit generates an appropriate gate control signal for the IGBT to operate during a fault current interruption process.

During normal operation, the main contact switch conducts the load current. When a short circuit fault occurs, the main contacts are separated by the solenoid/spring mechanism of the MCCB with an arc being generated across the contact gap. This arc voltage provides power to the self-power circuit, which subsequently activates the entire electronic circuit. A short moment later, the microswitch on the same moving arm and linked with the movement of the main contacts closes and sends a signal to the control and driver circuit to turn on the IGBT. At this point, the fault current is commutated from the mechanical to the electronic path, relieving the main contacts from the arcing stress. The control and timing circuit will then turn OFF the IGBT after a predefined short time duration, leaving the MOV to dissipate the residual electromagnetic energy in the electrical system. Finally, the isolation switch on the same moving mechanical arm and linked with the movement of the main contacts opens under a zero-current condition to provide galvanic isolation for the electronic circuit.

III. Modeling of EACB Operation

It is necessary to model and simulate the operation of EACB to gain a better understanding of the new breaker concept. In this section, the arc model of mechanical circuit breakers (MCBs) will be discussed first, followed by the modeling of EACB operation.

A. Arc Model of MCB

Limiting fault current by arc voltage is the most important aspect of EACB operation. To model this process, a model for MCB, including arcing, is needed. Several arc models were reported in the past [15], including Cassie arc model, Mayr arc model, Habedank arc model, and Schavemaker arc model, which are applicable under different conditions. Since the arc current is

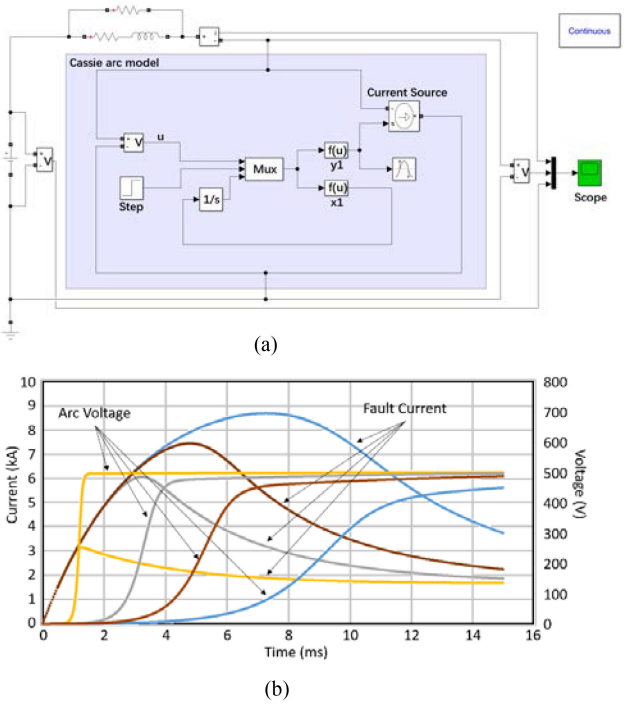

(a)

(b)

Fig. 4. (a) MATLAB Simulink model of an MCB based on Cassie arc model. (b) Simulated fault current and arc voltage waveforms for the CB with four different time constants of the Cassie arc model. Note that a smaller arc time constant leads to a faster rising arc voltage and a smaller peak fault current.

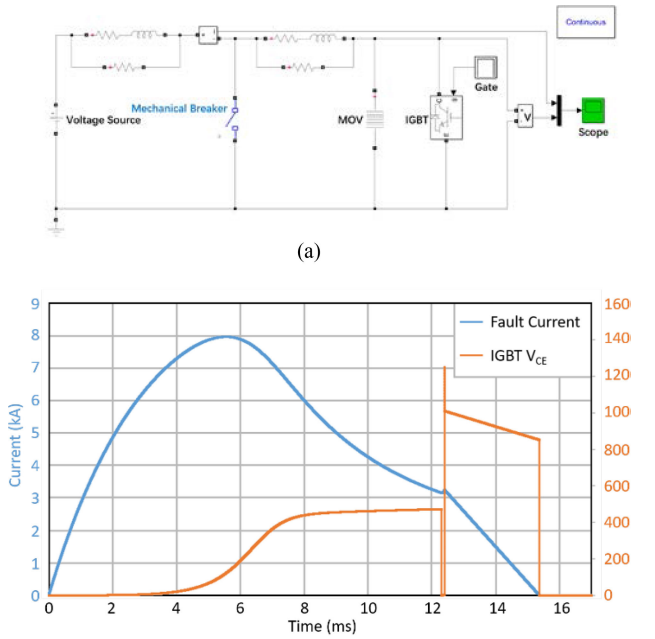

(a)

(b)

Fig. 5. (a) MATLAB Simulink model of the proposed EACB, including the MCB model shown in Fig. 4(a) and an IGBT and MOV. (b) Simulated fault current and IGBT (breaker) voltage waveforms of the EACB. Note that the IGBT only turns ON for 100 μs at $t = 12.3$ ms to aid the arc extinction in the mechanical contacts.

high (several kiloamperes) and the arc voltage is almost constant during the operation of the EACB, the Cassie arc model [16] is used in MATLAB SIMULINK simulation, as shown in Fig. 4(a). The Cassie arc model is expressed as

$$\frac{1}{u}\frac{dg}{dt} = \frac{1}{\tau}\left(\frac{u^2}{U_c^2} - 1\right) \tag{1}$$

where g is the conductance of the arc, τ is the arc time constant (unrelated to the time constant of the dc fault testing system mentioned later), U_c is the final constant arc voltage, and u is the arc voltage.

The measured waveforms of Fig. 1 can be qualitatively reproduced in simulation by selecting appropriate empirical model parameters. Fig. 4(b) shows the simulated fault current and arc voltage waveforms for the MCB with four different arc time constants (τ) in the Cassie arc model. Note that a smaller τ leads to a faster rising arc voltage and a smaller peak fault current. It is observed that the faster the arc voltage rises, the lower the peak fault current will be. In practice, the rate of arc voltage rise is determined by the separation speed of the metal contacts. It is therefore advantageous to design a mechanical breaker with a short opening time for an EACB. It is also observed that the simulated peak current and arc voltage are similar to those from the measurement data, but the simulated fault current downslope after peaking is more gradual than the experimental results. This may be because the arc voltage ripples in the actual testing circuit speed up the current decline process.

B. *Modeling of EACB Operation*

A Simulink model is further developed for EACB, as shown in Fig. 5(a), which incorporates the MCB model with embedded Cassie arc model with the appropriate parameters. The loop inductance and resistance, system voltage and current, MOV parameters, IGBT parameters, mechanical breaker parameters, and IGBT ON time can be varied in simulation to examine their influence on the EACB operation. The simulated breaker current and voltage waveforms for a 600-V dc voltage, a time constant of 3 ms, and an IGBT ON-time of 100 μs are shown in Fig. 5(b). These conditions are similar to the experimental setup of Fig. 1. At 12.3 ms, the IGBT turns ON to conduct about 3000-A fault current and relieve the mechanical breaker. After 100 μs, the IGBT turns OFF to interrupt the fault current. The parasitic inductance in the loop generates a voltage spike across the IGBT until the MOV clamps it. After about 3 ms, the electromagnetic energy stored in the loop is fully absorbed by the MOV and the fault interruption process is completed. This energy absorption time can also be adjusted in practical applications by selecting different MOVs. MOVs with higher clamping voltage can absorb the stored energy faster.

IV. Design Considerations

Several key considerations for designing an EACB are discussed in this Section IV-A, 600 V/250 A (nominal) EACB is designed for PV farm, EV charging station, and battery energy storage applications.

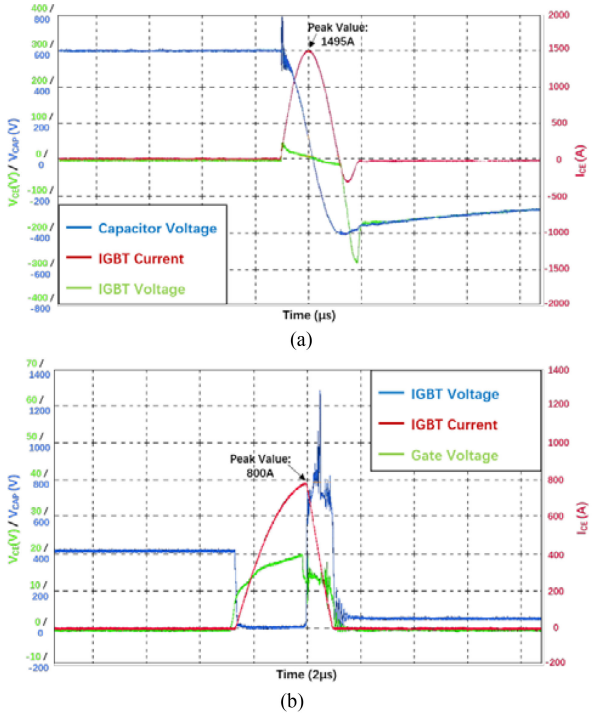

Fig. 6. Measured waveforms of the 1200 V/130 A rated IGBT in TO-247 package (IRG7PSH73K10). (a) Capacitor discharge surge current characterization test showing a peak current capability of 1495 A, the IGBT at a gate voltage of 30 V. (b) RBSOA test exhibiting the safe turnoff of the IGBT at 800 A/1200 V (comparing to 300 A/1200 V from datasheet) under clamped inductive switching conditions.

A. *Selection of Electronic Components*

An IGBT is selected as the main electronic switch to commutate the fault current. In order to provide enough assistance to the mechanical breaker during fault interruption, the IGBT needs to conduct a peak current of 2–3 kA for a period of 100–200 μs. This presents a major design challenge under the cost constraint. It would be cost prohibitive to use a kiloampere-rated IGBT power module for the EACB design. Alternatively, the feasibility of operating IGBTs up to 10X of their rated current in a short pulse mode (referred to as "extreme operation") was studied by the authors in [17].

Following the "extreme operation" design methodology, it is proposed to use only four 1200 V/130 A rated low-cost discrete IGBTs in TO-247 package in parallel for the EACB design. Fig. 6 shows the measured waveforms of a single IGBT (IRG7PSH73K10 [18]) during a capacitor discharge surge current test and a RBSOA test, respectively. The IGBT exhibits a peak current capability of 1495 A at a gate voltage of 30 V, more than 10X of its rated dc current of 130 A. The IGBT can also safely turns OFF a current of 800 A at a flyback voltage of 1200 V under the clamped inductive switching conditions, significantly higher than its 300 A/1200 V datasheet safe operating area (SOA) specifications.

An IGBT conducting a large current will generate a large amount of heat and reach a peak junction temperature of 175 °C rapidly. Transient thermal calculation is performed to estimate the maximum current for a certain pulsewidth for the IGBT extreme operation. Fig. 7 shows the calculated maximum

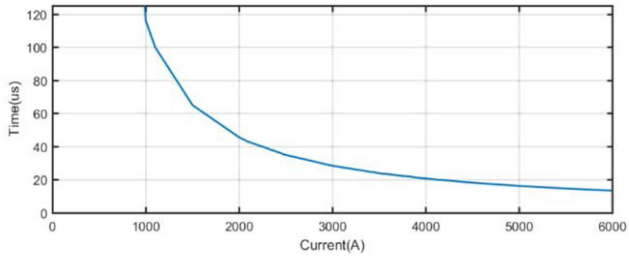

Fig. 7. Calculated maximum current versus time curve for the pulse operation of the 1200 V/130 A rated IGBT in TO-247 package (IRG7PSH73K10) imposed by thermal limitation ($T_{\mathrm{jmax}} \leq 175\,^{\circ}\mathrm{C}$ per datasheet specification).

pulsewidth as a function of current of the single IGBT, limited by T_{jmax} of 175 °C at room ambient temperature. It is seen that the discrete IGBT is allowed to conduct a pulse current of 1000 A for a duration over 100 μs. It is also experimentally demonstrated that the 1200 V/130 A IGBT (IRG7PSH73K10) can repeatedly conduct a pulse current of 1250 A for 100 μs at an ambient temperature of 25 °C [17]. With this result, four of the selected IGBTs in parallel can provide a pulse current capability over 4 kA, which is sufficient for the EACB operation.

The voltage rating of the electronic components, such as the IGBT, the MOV, the diode bridge, and the self-power circuit, is another important consideration. The IGBTs must have a voltage rating higher than the MOV maximum clamping voltage and the system bus voltage (600 V) to prevent breakdown failure during fault interruption. Two IGBT voltage ratings are considered in this study: 1200 and 1700 V. The MOV must have a nominal voltage higher than the bus voltage to prevent undesirable leakage current during nominal operation, but a clamping voltage at the IGBT turnoff lower than the IGBT breakdown voltage. It must be below the breakdown voltage of the mechanical gap to prevent arc reignition during the interruption process. Two MOV components are used in this study: Littelfuse V351HA40 (<894 V at 200 A) and V511HA40 (<1300 V at 200 A) for the 1200- and 1700-V IGBT, respectively [19]. The self-power supply circuit must operate in an input voltage range, the minimum arcing voltage and the maximum MOV clamping voltage.

In addition, the bidirectional capability also needs to be considered for the EACB design. This can be realized by using either a diode bridge with a single IGBT switch or two back-to-back IGBTs with two antiparallel diodes. The diode bridge and a single IGBT approach are selected for the EACB design because fewer IGBTs and gate drivers are required. The diode bridge needs to conduct the same fault current as the IGBT, thus, the same current capability calculation and component selection method used for IGBT should apply. Two types of diodes are selected in this study: VBO88-12NO7 (1200 V/90 A rating with 1000-A pulse capability) [20] and VBO88-12NO7 (1600 V/90 A rating with 1000-A pulse capability) [21] to work with the 1200- and 1700-V IGBTs, respectively.

B. *Control and Timing Circuit Design*

The control and timing circuit of the EACB needs to be carefully designed to turn ON the IGBT at the right time and for the right duration to ensure a successful fault current commutation

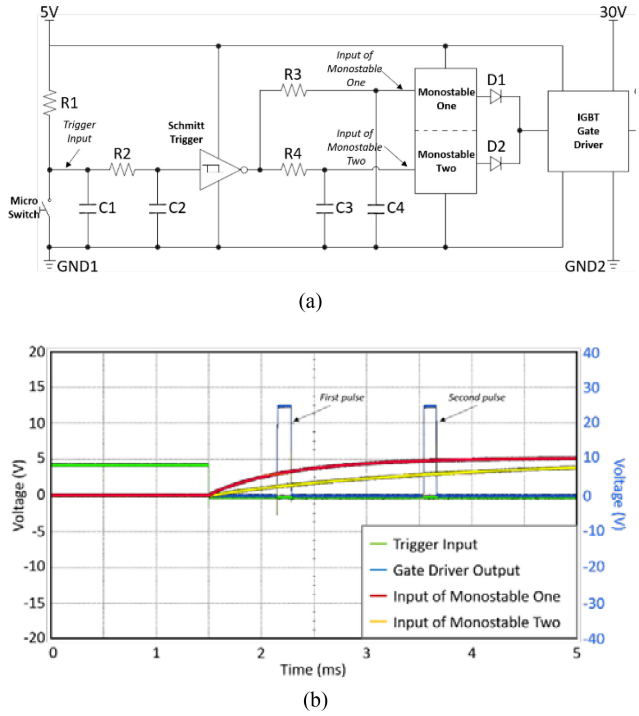

Fig. 8. Control circuit structure and measured signal processing of the circuit. The green step-down signal is the input trigger signal from microswitch, the red and yellow curves are the two input signal of the monostable multivibrator with different delay time, and the blue waveform is the output trigger signal, which contains two pulses with adjustable pre-set pulsewidth and delay time. (a) Schematic of the control and timing circuit. (b) Measured control signal waveforms.

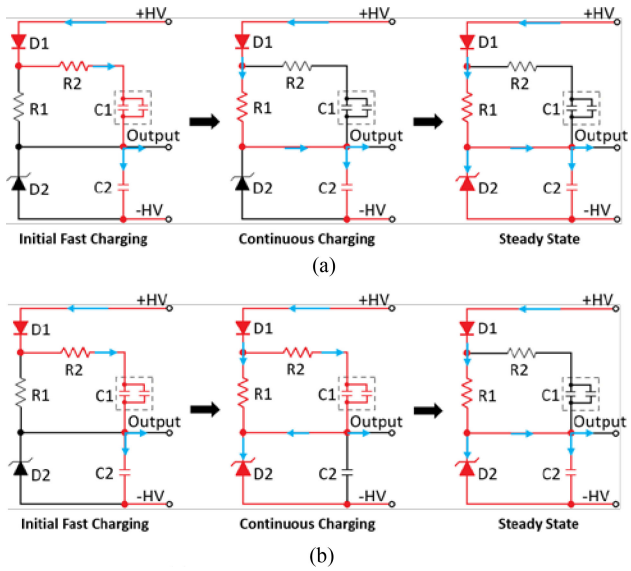

Fig. 9. Simplified circuit schematics of the self-power circuit showing three stages of operation for (a) low input voltage (<75 V) and (b) high input voltage (>75 V).

and interruption. The simplified schematics for the control and timing circuit and measured control signal waveforms are shown in Fig. 8(a) and (b), respectively. The control circuit comprises an input filter, a Schmitt trigger, two monostable multivibrators with their input *RC* delay circuits, and an IGBT gate driver.

The mechanical microswitch closes just a few milliseconds after the main contact switch opens in response to a fault condition and triggers the control and timing circuit. The filter circuit made of C1, C2, and R2, and the Schmitt trigger (SN74LVC2G14 from TI) are used for filtering out the input signal noising due to the bouncing of the microswitch. The two monostable multivibrators (CD14538B from TI) are used to generate two input pulses for the IGBT driver IC with adjustable pulsewidths for the best interruption performance. The first pulse is used to turn the IGBT ON and OFF for a preset time duration (typically 100–150 μs) for fault current commutation and interruption. There is a concern that the extinguished arc in the main contacts might be reignited when the breaker voltage increases rapidly with the IGBT turning OFF after the first pulse under certain circumstances. For this reason, the second pulse from the second monostable multivibrator is used as an optional safety measure to turn the IGBT ON and OFF for a second time. If there is no arc reignition in the main breaker, the second activation of the IGBT merely commutates the MOV current for a brief period and then turns OFF without further interference to the EACB interruption process. The *RC* delay circuits at the input of the multivibrators are used to provide the optimal timing of these two IGBT gate pulses, as shown in Fig. 8 (a). An isolated IGBT gate driver IC (Infineon's 1EDI60I12AF [22]) is selected for the EACB design, which has a typical drive current of 10 A and a maximum delay time of 330 ns and requires a supply voltage of 3–17 V on the input side and 13–35 V on the output side.

C. Self-Power Circuit Design

The main function of the self-power circuit is to extract power from the arc voltage across the main contacts (also in parallel with the IGBT and MOV) to generate a 5-V output for the control electronics and a 30-V output for the IGBT gate driver. Therefore, there is no need for external power supply to operate the EACB. The main challenge for designing the self-power circuit is to operate with an extremely wide input voltage range from a minimum arc voltage 30 V to a maximum MOV clamping voltage of 1500 V. In addition, the self-power circuit must continue supplying stable 5 V/30 V input voltages to the control electronics during the IGBT-ON duration when the "arc voltage" is only a few volts (i.e., the IGBT forward voltage drop). Fig. 9 shows the simplified circuit schematic of self-power circuit and different stages of the charging process under low (<75 V) and high input voltage (>75 V), respectively. Note that two of such circuits are needed for the 5-V output to the control electronics and the 30-V output to the IGBT driver, respectively. The circuit consists of two capacitors C1 and C2 in series for the initial fast charging (also through resistor R2) and voltage holding, a resistor R1 for continuous charging, and a Zener diode D2 for clamping the output voltage at the final steady stage when the input voltage tends to be high. The Zener diode D2 starts to clamp the output voltage and dissipating heat immediately after the initial fast charging phase for the high input voltage case while it only does so in the steady state for the low input voltage case. The values of the resistors and capacitors need to be optimally

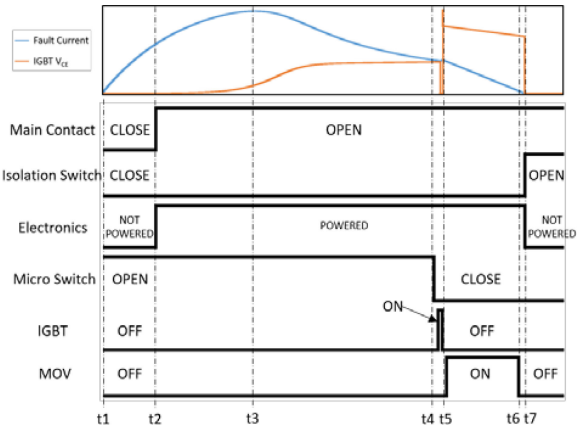

Fig. 10. Timing sequence of EACB operation in response to a fault condition (only one IGBT pulse is shown for the purpose of simplicity).

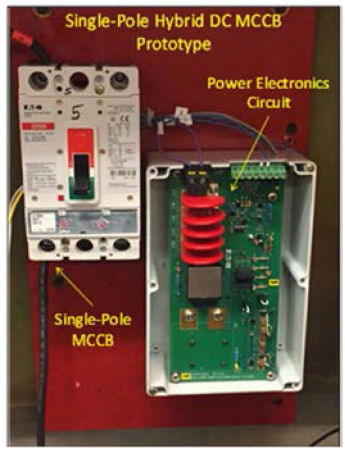

Fig. 11. Photographs of the 600VDC/250A EACB prototype and the commutation electronic circuit.

selected to quickly provide the desirable output voltage without overheating during the entire process of fault interruption. Improper component selection can cause problems, such as slow charging time or components damage during charging process. For example, R2 in series with C1 and C2 is used limit the inrush current in the beginning of the charging process. A large R2 will slow down the charging speed, but a too small R2 will allow a too large current through the Zener diode D2 during the continuous charging stage shown in Fig. 9(b) and may cause the burnout of D2. Obviously, the self-power circuit cannot operate for an extended time period under a high input voltage because of overheating of the circuit components, particularly the Zener diode D2. It is experimentally characterized that the self-power circuit has a safe operating time of 2.5 s at a dc voltage of 600 V and only 350 ms at 1500 V. Fortunately, the EACB only needs power for less than 10 ms, well within these safe time limits.

D. Timing Coordination Considerations

Fig. 10 conceptually depicts the timing sequence of EACB operation in response to a fault condition. The main contact switch initially conducts the load current with the microswitch being open, the isolation switch closed, and the electronic path completely inactive. When a short circuit fault occurs at t_1, the fault current through the main contacts rises rapidly. At t_2, the fault current becomes sufficiently high, and opens the main contacts by the solenoid/spring mechanism with an arc being generated across the contact gap. This arc voltage provides power to the self-power circuit, which subsequently activates the entire electronic path. The fault current reaches its peak and starts to decline at t_3. At t_4, the microswitch on the same moving arm and linked with the movement of the main contacts closes and sends a signal to the control and driver circuit. The delay time of t_2 to t_4 is determined by the mechanical design and the moving speed of the mechanical arm pulled by the spring mechanism. While these timing controls are not as precise as that of an electronic circuit, they are reasonably stable and repeatable. t_4 needs to be optimized for the purpose of effective and successful fault interruption. The main circuit breaker may be already damaged due to the excessive arcing heat if t_4 is too large. On the other hand, the IGBT may be destroyed by the excessive fault current if t_4 is too small. t_4 is typically set to 4–5 ms in this article. With a very short delay after t_4, the IGBT turns ON and commutates the fault current from the mechanical to the electronic path and relieve the main contacts from arcing stress. The control and timing circuit will then turn OFF the IGBT after a predefined short time duration of 100–150 μs at t_5, leaving the MOV to dissipate the residual electromagnetic energy in the electrical system between t_5 and t_6. The ON duration (t_5–t_4) of the IGBT is a tradeoff between the time required to relieve the metal contacts from the arcing stress and the time for the IGBT to reach a junction temperature of 175 °C. It is found that 100–150 μs is a good compromise. Finally, the isolation switch on the same moving mechanical arm and linked with the movement of the main contacts opens at t_7 under a zero-current condition to provide galvanic isolation for the electronic circuit. The total fault current interruption time of t_2 to t_7 mainly includes the contacts separation time and the MOV energy dissipation time and is roughly 5–6 ms in this work.

V. Experimental Results

Several 600 Vdc/250 A EACB prototypes are designed and built, as shown in Fig. 11. A commercial 600 Vac/250 A thermal-magnetic MCCB was modified to integrate the small isolation and microswitches onto the same pivoted mechanical arm where the main contact is linked to. The electronic circuit, also shown in Fig. 11, is prototyped on a 3oz copper PCB for high current capability. Table I lists the major electronic devices and specifications used in the EACB prototypes. Current sharing among the four IGBTs is addressed by carefully designing the PCB layout and using balancing gate resistors. The integrated electronic/mechanical EACB prototype is tested with a special 600 Vdc/10 kA power supply and a system time constant of 1 ms for dc current interruption capability characterization.

Fig. 12 shows the measured waveforms of the main (total) EACB current, the electronic branch current (IGBT and MOV combined), the breaker voltage (arc or IGBT/MOV voltage), the microswitch trigger signal, and the IGBT gate voltage. The

TABLE I
MAJOR ELECTRONIC COMPONENTS

Components	Model/Part #	Description	#
IGBT	IGW60T120	IGBT 1200V/100A TO247-3	4
MOV	V351HA40	Varistor 549.5V/40kA disc 40mm	5
Diode Bridge	VBO88-12NO7	Bridge rectifier diode 1.2kV/92A ECOPAC2	1
Gate Driver	1EDI60I12AF	IC IGBT driver 1200V, 6A DSO8	1
Schmitt Trigger	SN74LVC2G14	IC invert Schmitt 2channel SOT23-6	1
Monostable Multivibrator	CD14538B	IC multivibrator 100ns 16SOIC	1

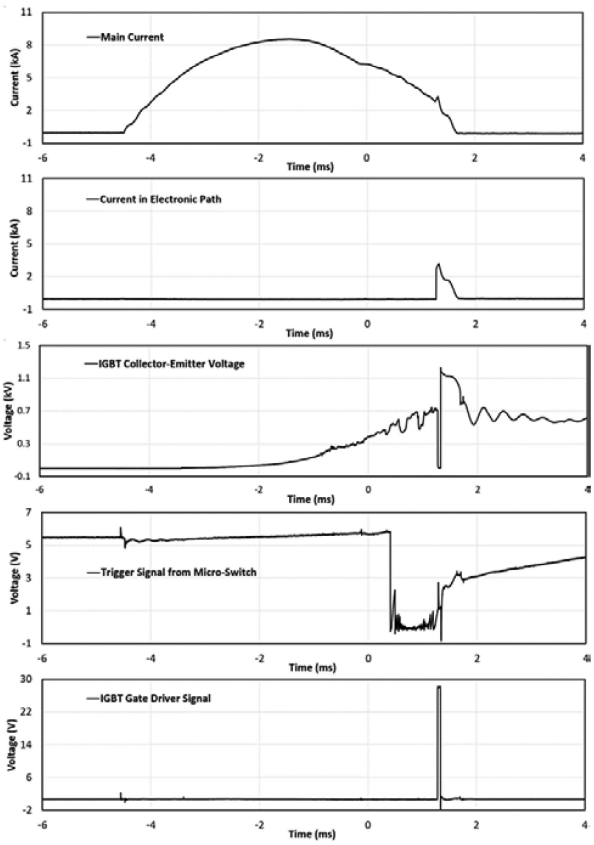

Fig. 12. Measured waveforms of EACB tested with a 600 Vdc/10 kA dc source: the main (total) EACB current, the electronic branch current (IGBT and MOV), the breaker voltage (arc or IGBT/MOV voltage), the microswitch trigger signal, and the IGBT gate voltage (from top down).

fault current start rising at time of –4.5 ms and reaches roughly 5 kA at –3.5 ms when the main contacts start separation with a gradually increasing arc voltage. The fault current reaches its peak value of 8.4 kA at –1.5 ms and starts decreasing because of the increasing arc voltage as a result of the widening contact gap. The arc chute of the mechanical breaker continues to remove the heat generated by the arc. At time of 0.5 ms, the microswitch opens and sends out a trigger signal to the control and timing electronics. After a prefixed delay of 0.7 ms, the IGBT turns ON at t of 1.2 ms and commutates the fault current (3.2 kA at

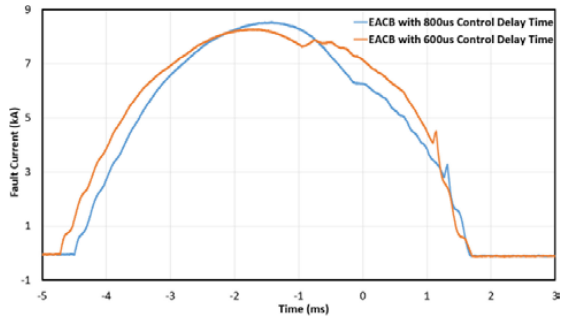

Fig. 13. Comparison of fault current waveforms between EACBs with a different control delay time setting of 0.8 and 0.6 ms, respectively.

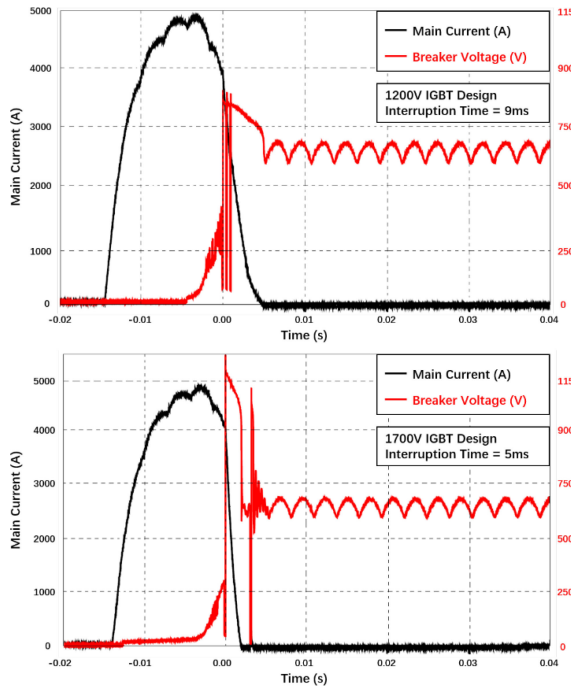

Fig. 14. Comparison of fault current and breaker voltage waveforms between 1200- and 1700-V EACB designs. The 1700-V design offers a much shorter energy dissipation time than the 1200-V design.

this moment) from the mechanical into the electronic path. After a period of 100 μs, the IGBTs turn OFF, and force the current flows into the MOVs. The EACB successfully completes the dc current interruption of 8.4 kA (peak) at 600 Vdc within 6 ms. In comparison, the same baseline ac circuit breaker fails to interrupt this level of dc current, as shown in Fig. 1.

These experimental results fully validate the EACB design concept and agree reasonably well with the modeling results. The influence of key EACB design parameters and system parameters on EACB operation is also investigated. Fig. 13 compares the fault current waveforms between two different control delay times of 0.8 and 0.6 ms, respectively. The fault current in the mechanical breaker commutates to the electronic path at 3 and 4.3 kA in these two cases, demonstrating the influence of the control delay time on the EACB behavior. Fig. 14 compares the breaker current and voltage waveforms between the two electronics designs with 1700- and 1200-V

IGBT and MOV ratings. It is clearly shown that the 1700-V design offers a much shorter energy dissipation time than the 1200-V design. For 1200-V IGBT design, the overall interruption time is about 9 ms and it takes the MOV 5 ms to dissipate all the residual energy. When the 1700-V IGBT is used, the total interruption time is around 5 ms and it take the MOV about 2.5 ms to dissipate the residual energy. The energy dissipated on the mechanical breaker, the IGBTs, and the MOVs during the fault current interruption process is also extracted from the current/voltage waveforms of Fig. 14(b) as 2777 J (43.8%), 21 J (0.3%), and 3543 J (55.9%), respectively. The MOVs and the metal contacts apparently are responsible for absorbing most of the electromagnetic energy in the circuit during the fault current interruption process. While the IGBTs only absorbs less than 1% of the total energy, their engagement with the right timing and duration has enabled the MCCB to interrupt a dc fault current, which it would be otherwise unable to do by itself. This indeed proves the fundamental concept of EACB.

VI. Conclusion

This article describes a new HCB concept termed EACB for low voltage dc power applications, such as EV charging infrastructures, PV farms, battery energy storage systems, and dc data centers. Several 600VDC/250A (nominal) EACB prototypes are designed and built, which experimentally demonstrate a dc fault current interruption capability of 8.4 kA at 600 V within 6 ms. Unlike other HCB concepts in the literature, the EACB uses a conventional thermal-magnetic MCCB baseline design with minimal modification, and an electronic commutation circuit, which needs to carry a relatively low fault current only for a very short duration ($\sim$100 μs), both contributing to significant cost savings. Discrete IGBTs are used in an ultrahigh current pulse mode in the EACB design as a cost-effective solution. Other advantages of the EACB include self-powered and autonomous operation, simple installation, inherently low on-resistance, and galvanic isolation. While an EACB does not facilitate arc-free or ultrafast breaking, it does provide a simple and cost-effective way to enhance the dc current interruption capability of conventional ac thermal-magnetic MCCB currently dominating the low voltage circuit breaker market. The limitations of the EACB concept include moderate response time (5–10 ms) and a limited lifetime ($>$10 operations) since it still relies on the arcing process, albeit electronically reduced, to interrupt the fault current and absorb electromagnetic energy.

Acknowledgment

This article is an extension of the conference paper "Electronically Assisted Circuit Breaker (EACB) for DC Power Systems," presented at the 10th IEEE Energy Conversion Congress and Expo (ECCE), 2019.

References

[1] M. Saeedifard, M. Graovac, R. F. Dias, and R. Iravani, "DC power systems: Challenges and opportunities," in *Proc. IEEE Power Energy Soc. General Meeting*, 2010, pp. 1–7.

[2] T. Dragicevic, J. C. Vasquez, J. M. Guerrero, and D. Skrlec, "Advanced LVDC electrical power architectures and microgrids: A step toward a new generation of power distribution networks," *IEEE Electrific. Mag.*, vol. 2, no. 1, pp. 54–65, Mar. 2014.

[3] D. Salomonsson and A. Sannino, "Low-voltage DC distribution system for commercial power systems with sensitive electronic loads," *IEEE Trans. Power Del.*, vol. 22, no. 3, pp. 1620–1627, Jul. 2007.

[4] H. Pugliese and K. Michael Von, "Discovering DC: A primer on DC circuit breakers, their advantages, and design," *IEEE Ind. Appl. Mag.*, vol. 19, no. 5, pp. 22–28, Sep./Oct. 2013.

[5] G. Li *et al.*, "Frontiers of DC circuit breakers in HVDC and MVDC systems," in *Proc. IEEE Conf. Energy Internet Energy Syst. Integr.*, 2017, pp. 1–6.

[6] H.-K. Cho, E.-W. Lee, and J.-H. Jeong, "DC arc extinction using external magnetic field in switching device," in *Proc. 6th Int. Conf. Elect. Mach. Syst.*, 2003, pp. 929–932.

[7] B. Pauli, G. Mauthe, E. Ruoss, G. Ecklin, J. Porter, and J. Vithayathil, "Development of a high current HVDC circuit breaker with fast fault clearing capability," *IEEE Trans. Power Del.*, vol. 3, no. 4, pp. 2072–2080, Oct. 1988.

[8] Z. J. Shen, Z. Miao, and A. M. Roshandeh, "Solid state circuit breakers for DC micrgrids: Current status and future trends," in *Proc. IEEE 1st Int. Conf. DC Microgrids*, 2015, pp. 228–233.

[9] A. M. S. Atmadji and J. G. J. Sloot, "Hybrid switching: A review of current literature," in *Proc. Int. Conf. Energy Manage. Power Del.*, Mar. 1998, vol. 2, pp. 683–688.

[10] K. Tahata *et al.*, "HVDC circuit breakers for HVDC grid applications," in *Proc. 11th IET Int. Conf. AC DC Power Transmiss.*, 2015, pp. 1–9.

[11] J. Zyborski, T. Lipski, J. Czucha, and S. Hasan, "Hybrid arcless low-voltage AC/DC current limiting interrupting device," *IEEE Trans. Power Del.*, vol. 15, no. 4, pp. 1182–1187, Oct. 2000.

[12] C. Peng, I. Husain, A. Q. Huang, B. Lequesne, and R. Briggs, "A fast mechanical switch for medium-voltage hybrid DC and AC circuit breakers," *IEEE Trans. Ind. Appl.*, vol. 52, no. 4, pp. 2911–2918, Jul./Aug. 2016.

[13] J. Meyer and A. Rufer, "A DC hybrid circuit breaker with ultra-fast contact opening and integrated gate-commutated thyristors (IGCTs)," *IEEE Trans. Power Del.*, vol. 21, no. 2, pp. 646–651, Apr. 2006.

[14] Y. Feng, Y. Zhou, Z. J. Shen, X. Zhou, and S. Krstic, "Electronically assisted circuit breaker (EACB) for DC power systems," in *Proc. 10th IEEE Energy Convers. Congr. Expo.*, 2019, pp. 2419–2425.

[15] R. F. Ammerman, T. Gammon, P. K. Sen, and J. P. Nelson, "DC-arc models and incident-energy calculations," *IEEE Trans. Ind. Appl.*, vol. 46, no. 5, pp. 1810–1819, Sep./Oct. 2010.

[16] K.-J. Tseng, Y. Wang, and D. M. Vilathgamuwa, "An experimentally verified hybrid Cassie-Mayr electric arc model for power electronics simulations," *IEEE Trans. Power Electron.*, vol. 12, no. 3, pp. 429–436, May 1997.

[17] Y. Feng, T. Liu, Z. A. Daniyal, A. M. Roshandeh, and Z. J. Shen, "Extreme operation of IGBTs," in *Proc. IEEE Transp. Electrific. Conf. Expo.*, 2017, pp. 269–274.

[18] "Insulated gate bipolar transistor," Infineon, Neubiberg, Germany, IRG7PSH73K10PbF datasheet, Sep. 2010.

[19] "Metal-oxide varistors (MOVs) industrial high energy terminal varistors," Littelfuse, Chicago, IL, USA, HA Varistor Series datasheet, Sep. 2017.

[20] "Standard rectifier module," IXYS, Milpitas, CA, USA, VBO88-12NO7 datasheet, Mar. 2013.

[21] "Standard rectifier module," IXYS, Milpitas, CA, USA, VBO88-16NO7 datasheet, Mar. 2013.

[22] "1EDI EiceDRIVER compact separate output variant for IGBT," Infineon, Neubiberg, Germany, 1EDI40I12AF datasheet, Nov. 2014.

[23] X. Zhou, Y. Feng, Z. John Shen, and S. Krstic, "Hybird DC molded case circuit breaker technology," in *Proc. 66th IEEE Holm Conf.*, 2017, pp. 1–9.

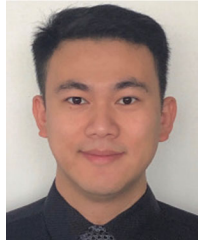

Yanjun Feng (Member, IEEE) received the B.S. degree from Donghua University, Shanghai, China, in 2013, the M.S. and Ph.D. degrees from the Illinois Institute of Technology, Chicago, IL, USA, in 2015 and 2019, respectively, all in electrical engineering.

He is currently with Canoo EV, Torrance, CA, USA. His research interests include hybrid circuit breakers and EV drivetrain power electronics. He has also authored/coauthored several papers on these topics.

Xin Zhou (Senior Member, IEEE) received the Ph.D. degree in mechanical engineering from the University of Minnesota, Minneapolis, MN, USA, in 1995.

From 1995 to 1996, he was with Phoenix Solutions Company, as a Plasma Technology Specialist, responsible for developing and designing plasma torch systems for waste remediation. He is currently an Engineering Manager with the Power Component Division, Eaton Corporation, Pittsburgh, PA, USA. He holds 72 U.S. patents and authored/coauthored more than 41 journal and conference papers. His research projects include arcing phenomena, next generation product development in power control and distribution, optical emission spectroscopy, and plasma-enhanced material processing.

Dr. Zhou was the recipient of the Eaton Innovation Award for both 2008 and 2010, and the Eaton Engineer of the Year Award for 2011. He has served as the Chair or member of various committees of IEEE Holm Conference. He was a recipient of the IEEE-CHMT Graduate Fellowship Award for Research on Electric Contacts for 1991–1992. He was also the recipient of the IEEE Erle Shobert Prize Paper Awards in 1993, 2003, 2011, and 2013.

Slobodan Krstic (Member, IEEE), photograph and biography not available at the time of publication.

Yuanfeng Zhou (Student Member, IEEE) received the B.S. degree in electrical engineering from Xi'an Jiaotong University, Xi'an, China, in 2009, and the M.S. degree from the Huazhong University of Science and technology, Wuhan, China, in 2012. He is currently working toward the Ph.D. degree with the Department of Electrical and Computer Engineering, Illinois Institute of Technology, Chicago, IL, USA.

From 2012 to 2015, he was with Emerson Network Power, Shenzhen, China, as a Design Engineer. His research interests, which include dc solid state circuit breakers, hybrid circuit breakers, and wide bandgap power electronics. He has also authored/coauthored more than ten papers on these topics.

Zheng John Shen (Fellow, IEEE) received the B.S. degree from Tsinghua University, Beijing, China, in 1987, and the M.S. and Ph.D. degrees from Rensselaer Polytechnic Institute, Troy, NY, USA, in 1991 and 1994, respectively, all in electrical engineering.

Between 1994 and 1999, he held a variety of positions, including Senior Principal Staff Scientist with Motorola. He was on the Faculty of the University of Michigan-Dearborn, from 1999 to 2004, and the University of Central Florida, from 2004 to 2012. He also served as a Board Member and Chief Scientist of GWS Semiconductor, Tempe, AZ, USA (now a division of Renesas Electronics) from 2002 to 2012, responsible for developing megahertz-frequency lateral power MOSFET technology for supercomputer and server applications. In 2013, he joined the Illinois Institute of Technology, as Grainger Chair Professor in electrical and power engineering. His research interests include power electronics, power semiconductor devices and ICs, automotive electronics, and renewable and alternative energy systems. He has also authored/coauthored more than 300 journal and conference articles, and holds 18 issued and several pending U.S. patents in these topics.

Dr. Shen was the recipient of the 2012 IEEE Region 3 Outstanding Engineer Award, the 2003 NSF CAREER Award, and two IEEE Transactions Paper Awards. He has been an active volunteer in the IEEE Power Electronics Society, and has served as VP of Products, AdCom Member, and the General Chair or Technical Program Chair of several major IEEE conferences, including ECCE and ISPSD. He is a fellow of the U.S. National Academy of Inventors.